Communication

# Evidence for Dynamics on a 100 ns Time Scale from Single- and Double-Quantum Nitrogen-14 NMR in Solid Peptides

Simone Cavadini, Anuji Abraham, Simone Ulzega, and Geoffrey Bodenhausen

*J. Am. Chem. Soc.*, **2008**, 130 (33), 10850-10851 • DOI: 10.1021/ja802603q • Publication Date (Web): 23 July 2008



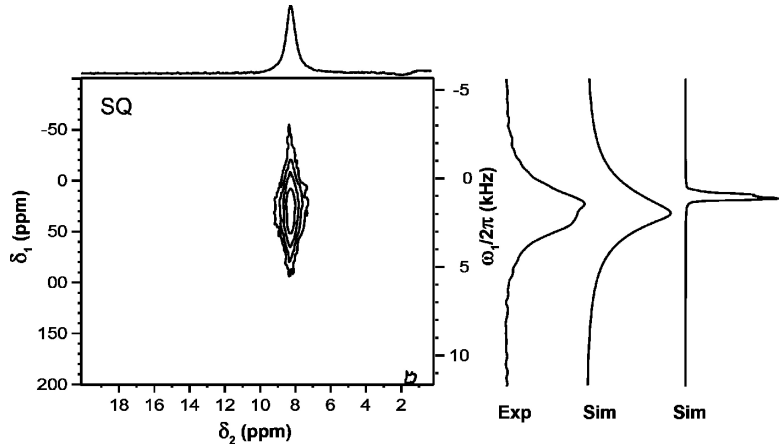


## More About This Article

Additional resources and features associated with this article are available within the HTML version:

- Supporting Information
- Links to the 1 articles that cite this article, as of the time of this article download
- Access to high resolution figures
- Links to articles and content related to this article
- Copyright permission to reproduce figures and/or text from this article

View the Full Text HTML

J|A|C|S
COMMUNICATIONS

Published on Web 07/23/2008

# Evidence for Dynamics on a 100 ns Time Scale from Single- and Double-Quantum Nitrogen-14 NMR in Solid Peptides

Simone Cavadini,[†] Anuji Abraham,*[,†] Simone Ulzega,[†] and Geoffrey Bodenhausen[†,‡]

*Laboratoire de Résonance Magnétique Biomoléculaire, Ecole Polytechnique Fédérale de Lausanne, Batochime, CH-1015 Lausanne, Switzerland, and Département de Chimie, associé au CNRS, Ecole Normale Supérieure, 24 rue Lhomond 75231, Paris Cedex 05, France*

Received April 9, 2008; E-mail: anuji.abraham@epfl.ch

Solid state NMR is an attractive tool to probe subtle dynamic processes[1–6] such as librational motions or hopping between conformations on micro- to millisecond time scales. Quadrupolar nuclei such as $^2$H and $^{14}$N ($I = 1$) are particularly suitable to monitor dynamics[1] because of their quadrupolar interactions ($0.1 < C_Q < 3$ MHz). Recently, it has been shown that dynamics can be characterized by comparing single- and double-quantum (SQ and DQ) deuterium ($^2$H) NMR spectra recorded with magic angle spinning (MAS).[3,5] The natural abundance of $^{14}$N is 99.6%, yet $^{14}$N spectroscopy was regarded as a difficult challenge until recently.[7–10] It has now become possible to observe $^{14}$N in solids by indirect detection[11–18] via "spy" nuclei with $S = 1/2$ such as $^{13}$C or $^1$H, in the manner of heteronuclear multiple-quantum correlation (HMQC).[19,20] The transfer of coherence from protons to $^{14}$N and vice versa can be achieved via second-order quadrupole−dipole cross terms,[12,16] via scalar couplings,[11,13] or via recoupled heteronuclear dipolar interactions,[17,18] notably by using symmetry-based RN sequences[21,22] of the type $R12_3^5$.

In the present study, the dynamics in a polycrystalline sample of the tripeptide Ala-Ala-Gly (AAG) were studied by analyzing proton-detected SQ and DQ $^{14}$N spectra without replacing any protons by $^2$H nuclei. The three rapidly hopping protons of the $-NH_3^+$ group and the two relatively rigid NH pairs in AAG give rise to only three signals in Figure 1. The $^{14}$N quadrupolar couplings were estimated to be $C_Q = +1.13$ and $-3.21$ MHz and the asymmetry parameters $\eta_Q = 0.28$ and 0.32 for the nitrogen nuclei in the $-NH_3^+$ group (peak I in Figure 1) and the two (degenerate) amide groups (peak II), respectively.[18] The SQ spectrum of the $-NH_3^+$ group in Figure 1a features significant broadening in comparison to the static simulation of Figure 1c. This stands in contrast to glycine[13] and alanine,[12] where fast hopping of the $-NH_3^+$ protons leads to a partial averaging of the $^{14}$N quadrupolar couplings.[12,13] It cannot be excluded that the analogous rotation in AAG is slower,[23] so that incomplete averaging of the $^{14}$N quadrupolar coupling would leave some residual line broadening. However, there may be other motions in the environment of the $^{14}$N nucleus that affect the orientation and/or principal values of the quadrupole tensor, e.g., motions of charges (possibly protons) and rotations of methyl or other ammonium groups. Jumps in the first-order quadrupole splitting interfere with the averaging of the SQ spectrum under MAS. To explore this hypothesis, we simulated ±5° jumps about the *yy* axis of the quadrupole tensor. The slight asymmetry of the line shape in Figure 1a can be attributed to nonuniform excitation of the crystallites, the radio frequency pulses being much weaker than the quadrupole splitting. Polymorphism can be ruled out since the $^{13}$C spectrum of $^{13}C^{\alpha}$-enriched AAG shows only three clean peaks. By contrast, the DQ $^{14}$N spectrum of the $-NH_3^+$ group in AAG (peak I in Figure 1d,e) is not significantly affected by motions. For DQ $^{14}$N spectra, MAS merely serves to remove weak dipolar couplings to remote spins. Therefore, motions do not lead to significant line broadening in DQ spectra. Similar effects were shown for $^2$H by Ashbrook et al.[3] and Cutajar et al.[5]

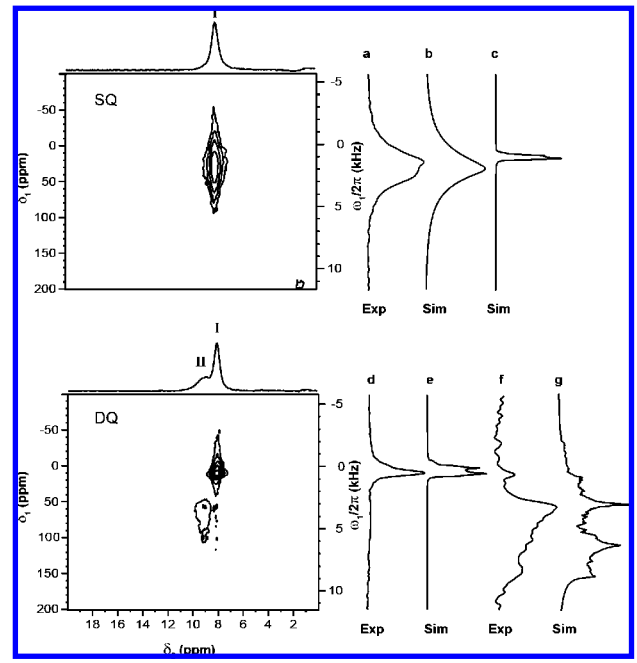


***Figure 1.*** Experimental SQ (top) and DQ (bottom) $^{14}$N/$^1$H correlation spectra of the $-NH_3^+$ group (I) and the two relatively rigid amide NH pairs that contribute to peak II in the tripeptide AAG. An 11 $\mu$L sample in a 2.5 mm rotor was spun at 29.76 kHz in a static field of 18.8 T (57.8 and 800 MHz for $^{14}$N and $^1$H) at 49 °C, estimated according to Langer et al.[24] The radio frequency (RF) amplitudes were $\nu_1(^1H)_{\pi/2} = \nu_1(^1H)_{\pi} = 100$ kHz and $\nu_1(^1H)_{RN} = 59.52$ kHz during the excitation and the refocusing intervals $\tau_{exc} = \tau_{rec} = 100.8$ $\mu$s of the HMQC sequence.[18] The windowless recoupling sequence[22] $R12_3^5$ applied to the $^1$H spins consisted of six times $\{180_{75}\ 180_{285}\}$, i.e., six pairs of $\pi$ pulses with phases $\phi = 75$ and 285° or $12\pi$ pulses in three rotor periods. With $\nu_1(^{14}N) = 80$ kHz, the optimum $^{14}$N pulse lengths were $\tau_p = 20$ and 26 $\mu$s, respectively, for the SQ and DQ spectra. (a) Experimental cross section parallel to the $\omega_1$ dimension of the SQ spectrum of site I. (b) Simulated SQ response for a ±5° two-site jump, calculated as explained in the text. (c) Simulated SQ spectrum obtained without internal motions. (d,f) Experimental cross sections parallel to the $\omega_1$ dimension of the DQ spectrum of sites I and II. (e,g) Simulated DQ spectra of sites I and II, without motions. All simulations included 28 656 crystallite orientations. The vertical $\omega_1$ axis was calibrated to 0 ppm for $^{14}NH_4Cl$. The spectra were acquired with a $^{14}$N offset with respect to $^{14}NH_4Cl$ of $\Omega^I = 10$ kHz for SQ and 1 kHz for DQ. The 2D spectra resulted from averaging 256 (SQ) and 512 (DQ) transients for each of 100 $t_1$ increments with $\Delta t_1 = 1/\nu_{rot} = 33.6$ $\mu$s, and a relaxation interval of 10 s.

To ascertain the effects of motions on $^{14}$N spectra, numerical simulations were carried out in the manner of McConnell,[25–28]

[†] Ecole Polytechnique Fédérale de Lausanne.
[‡] Ecole Normale Supérieure.


10.1021/ja802603q CCC: $40.75 

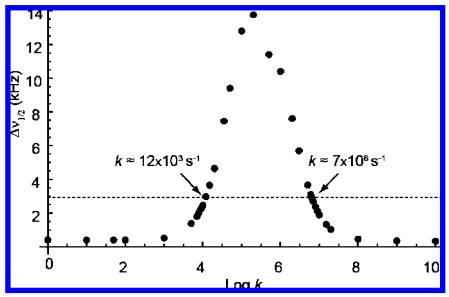


***Figure 2.*** Simulations of the full line width at half-height $\Delta\nu_{1/2}$ of SQ $^{14}$N spectra as a function of the exchange rate $k$, assuming a two-site jump about the $yy$ axis of the quadrupole tensor through ±5°, $C_Q = 1.13$ MHz, $\eta_Q = 0.28$, and 28 656 different crystallite orientations, under the assumption of uniform excitation of the crystallites. Only about 0.4 kHz of the width are due to the second-order quadrupole splitting as shown in the static simulation of Figure 1c. This width does not depend on the RF field amplitude between 140 and 80 kHz and increases by about 0.2 kHz at 40 kHz. A similar curve is obtained for 120° hops around a $zz$ axis that is assumed to be parallel to the C−N bond. The dashed horizontal line represents the width $\Delta\nu_{1/2} \approx 3$ kHz of the experimental SQ spectrum of Figure 1a, after subtracting 0.2 kHz due to proton−proton dipolar interactions determined from proton echo experiments which gave $T_2'(^1\mathrm{H}) = 1.6$ ms.

considering a symmetrical chemical exchange between two equally populated sites with a first-order rate $k$. In the presence of MAS, the spin dynamics is governed by a time-dependent Liouville equation which can be solved numerically by dividing each rotor period into 10 equally spaced intervals and calculating the propagator in a stepwise manner. Smaller increments do not affect the outcome. Equation 1 shows the Wigner transformations of the principal axes systems (PAS) of the electric field gradient (EFG) tensors of the two sites to a common laboratory (Lab) frame where

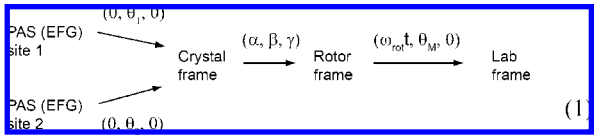


$(\alpha, \beta, \gamma)$ define the crystallite orientations, $\omega_{rot}$ is the spinning frequency, and $\theta_M$ is the magic angle. Figure 2 shows the full line widths at half-height $\Delta\nu_{1/2}$ calculated as a function of the exchange rate $k$. The numerical simulations match the experimental SQ line shapes ($\Delta\nu_{1/2}^{exp} \approx 3$ kHz) for $k \approx 10^4$ or $10^7$ s$^{-1}$. To discriminate between these two possible regimes, SQ experiments were performed at different sample temperatures (Figure 3). It was found that the line width decreases with increasing temperature. This excludes the regime near $k \approx 10^4$ s$^{-1}$ and proves that the motions must occur at $k \approx 10^7$ s$^{-1}$. The line width contribution of the homonuclear proton−proton dipolar interactions can be determined from proton echo experiments: $T_2'(^1\mathrm{H}) = 1.6$ ms (0.2 kHz) for the $-NH_3^+$ peak at 48 °C with 29.76 kHz MAS. This contribution is negligible compared to the line broadening induced by dynamic processes, which is ∼2−3 kHz between 29 and 48 °C. Small errors in line widths do not lead to significant changes in the estimates of $k$. The SQ $^{14}$N responses of the two amide NH groups in AAG, which have much larger quadrupole couplings than the $-NH_3^+$ group, cannot be observed in Figure 1 (top), presumably because of inefficient SQ excitation and/or dynamic effects. However, the (superimposed) DQ $^{14}$N responses of the two NH amide groups can be readily observed (peak II in Figure 1f) since the DQ line widths are hardly affected by motions, and the excitation is less critical.[16] This DQ spectrum allowed us to estimate that $C_Q \approx -3.21$ MHz for both amide NH groups in AAG.

In summary, the indirect detection of $^{14}$N spectra via protons in the manner of HMQC allows one to obtain SQ and DQ $^{14}$N spectra

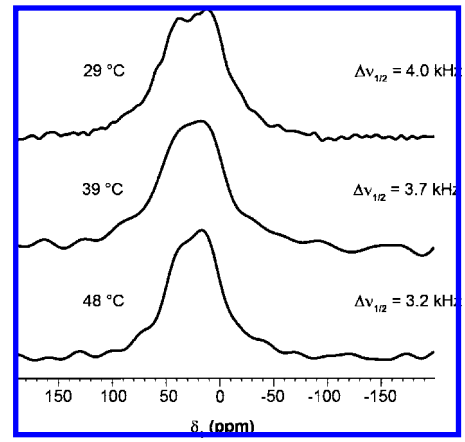


***Figure 3.*** Experimental SQ $^{14}$N spectra of the $-NH_3^+$ group of AAG spinning at 29.76 kHz in a static field of 18.8 T (57.8 and 800 MHz for $^{14}$N and $^1$H). The air drive temperatures were corrected according to Langer et al.[24] The experimental parameters are as in Figure 1 except the number of scans, which was 32 for the middle and bottom spectra.

in solids, and the comparison of the line widths with simulations reveals motions in the tripeptide AAG with rates on the order of $10^7$ s$^{-1}$ at 49 °C. This regime was hitherto not accessible to any methods that afford atomic resolution.

**Acknowledgment.** We are indebted to Dr. Luminita Duma for valuable comments. This work was supported by the Fonds National de la Recherche Scientifique (FNRS) and the Commission pour la Technologie et l'Innovation (CTI), Switzerland.

## References

(1) Long, J. R.; Sun, B. Q.; Bowen, A.; Griffin, R. G. *J. Am. Chem. Soc.* **1994**, *116*, 11950.
(2) Kristensen, J. H.; Hoatson, G. L.; Vold, R. L. *Solid State Nucl. Magn. Reson.* **1998**, *13*, 1.
(3) Ashbrook, S. E.; Antonijevic, S.; Berry, A. J.; Wimperis, S. *Chem. Phys. Lett.* **2002**, *364*, 634.
(4) Kotecha, M.; Chaudhuri, S.; Grey, C. P.; Frydman, L. *J. Am. Chem. Soc.* **2005**, *127*, 16701.
(5) Cutajar, M.; Ashbrook, S. E.; Wimperis, S. *Chem. Phys. Lett.* **2006**, *423*, 276.
(6) Thrippleton, M. J.; Cutajar, M.; Wimperis, S. *Chem. Phys. Lett.* **2008**, *452*, 233.
(7) Proctor, W. G.; Yu, F. C. *Phys. Rev.* **1950**, *77*, 717.
(8) Stark, R. E.; Haberkorn, R. A.; Griffin, R. G. *J. Chem. Phys.* **1978**, *68*, 1996.
(9) Jakobsen, H. J.; Bildsoe, H.; Skibsted, J.; Giavani, T. *J. Am. Chem. Soc.* **2001**, *123*, 5098.
(10) Tycko, R.; Stewart, P. L.; Opella, S. J. *J. Am. Chem. Soc.* **1986**, *108*, 5419.
(11) Gan, Z. *J. Am. Chem. Soc.* **2006**, *128*, 6040.
(12) Cavadini, S.; Lupulescu, A.; Antonijevic, S.; Bodenhausen, G. *J. Am. Chem. Soc.* **2006**, *128*, 7706.
(13) Cavadini, S.; Antonijevic, S.; Lupulescu, A.; Bodenhausen, G. *J. Magn. Reson.* **2006**, *182*, 168.
(14) Gan, Z. *J. Magn. Reson.* **2006**, *183*, 235.
(15) Gan, Z. *J. Magn. Reson.* **2006**, *184*, 39.
(16) Cavadini, S.; Antonijevic, S.; Lupulescu, A.; Bodenhausen, G. *ChemPhysChem* **2007**, *8*, 1363.
(17) Gan, Z.; Amoureux, J. P.; Trébosc, J. *Chem. Phys. Lett.* **2007**, *435*, 163.
(18) Cavadini, S.; Abraham, A.; Bodenhausen, G. *Chem. Phys. Lett.* **2007**, *445*, 1.
(19) Müller, L. *J. Am. Chem. Soc.* **1979**, *101*, 4481.
(20) Iuga, D.; Morais, C.; Gan, Z.; Neuville, D. R.; Cormier, L.; Massiot, D. *J. Am. Chem. Soc.* **2005**, *127*, 11540.
(21) Carravetta, M.; Eden, M.; Zhao, X.; Brinkmann, A.; Levitt, M. H. *Chem. Phys. Lett.* **2000**, *321*, 205.
(22) Brinkmann, A.; Levitt, M. H. *J. Chem. Phys.* **2001**, *115*, 357.
(23) Williams, M. A. K.; Keenan, R. D.; Halstead, T. K. *Solid State Nucl. Magn. Reson.* **1996**, *6*, 47.
(24) Langer, B.; Schnell, L.; Spiess, H. W.; Grimmer, A. R. *J. Magn. Reson.* **1999**, *138*, 182.
(25) McConnell, H. M. *J. Chem. Phys.* **1958**, *28*, 430.
(26) Helgstrand, M.; Härd, T.; Allard, P. *J. Biomol. NMR* **2000**, *18*, 49.
(27) Larsen, F. H. *J. Magn. Reson.* **2004**, *171*, 293.
(28) Larsen, F. H. *Solid State Nucl. Magn. Reson.* **2007**, *31*, 100.

JA802603Q